Available online at www.sciencedirect.com
ScienceDirect
Journal of Power Sources 174 (2007) 872–876
JOURNAL OF POWER SOURCES
www.elsevier.com/locate/jpowsour

Short communication

Modeling lithium/hybrid-cathode batteries

Parthasarathy M. Gomadam [a,*], Don R. Merritt [a], Erik R. Scott [a], Craig L. Schmidt [a], Paul M. Skarstad [a], John W. Weidner [b]

[a] *Medtronic Energy and Component Center, 6700 Shingle Creek Pkwy, Brooklyn Center, MN 55430, United States*
[b] *Center for Electrochemical Engineering, Department of Chemical Engineering, University of South Carolina, Columbia, SC 29208, United States*

Available online 29 June 2007

Abstract

This document describes a first-principles-based mathematical model developed to predict the voltage–capacity behavior of batteries having hybrid cathodes comprising a mixture of carbon monofluoride (CF_x) and silver vanadium oxide (SVO). These batteries typically operate at moderate rates of discharge, lasting several years. The model presented here is an accurate tool for design optimization and performance prediction of batteries under current drains that encompass both the application rate and accelerated testing.

Keywords: Hybrid batteries; Carbon monofluoride, CFx; Silver vanadium oxide, SVO; Lithium primary battery; Mathematical model

1. Background

Lithium/hybrid-cathode primary battery technology, developed by Medtronic for implantable medical devices, uses a cathode mixture of carbon monofluoride (CF_x) and silver vanadium oxide (SVO) [1–5]. The two materials combine in a synergistic fashion to give improved performance compared to either pure-component used alone. For a given volume, CF_x provides high energy but lower power, whereas SVO provides high power but only moderate energy. A mixture of the two materials, consequently, gives higher energy than SVO, and higher power than CF_x. In addition, the mixture allows a low-voltage plateau at high depth-of-discharge (DOD), which provides a reliable end-of-service warning.

Hybrid cathodes are designed at various mix-ratios (the ratio of the capacities delivered by the cathode due to CF_x and SVO), thicknesses, porosities, and surface areas to match performance characteristics to device operating conditions. These characteristics include: energy density, power density and the shape of the voltage–capacity curve near the end of discharge. To facilitate the design process, a physically-based mathematical model of the hybrid cathode is developed that predicts cathode performance over a range of design parameters and operating conditions applicable to the devices that use these batteries.

2. Model development

Fig. 1 is a schematic representation of a typical hybrid-cathode battery from a modeling perspective. The cathode is a porous pellet made of CF_x, SVO, and inert materials in varying proportions and pressed on to the current collector. The separator is an inert porous material such as polyethylene, while the anode is Li metal pressed onto a current collector. The pores of the cathode and separator are flood-filled with electrolyte, and excess electrolyte fills the headspace and other voids in the can. Electrochemical oxidation of Li to Li^+ ions occurs at the anode/electrolyte interface, driving ionic current flow from the anode to the cathode, where electrochemical reduction of CF_x and SVO take place. In contrast to the anode, the sites of cathode reaction are its pore-walls, which are distributed throughout the volume of the porous cathode. The electrons generated due to oxidation at the anode and consumed due to reduction at the cathode drive current in the external circuit, which powers the device.

The following assumptions have been made in developing the models for hybrid batteries:

1. Cathode limits cell capacity (i.e., excess Li in anode).
2. Cathode dominates cell resistance (i.e., resistances in anode, separator etc. are negligible).
3. Cathode is kinetically limited (i.e., ohmic resistances are negligible).

* Corresponding author.
E-mail address: partha.m.gomadam@medtronic.com (P.M. Gomadam).

0378-7753/$ – see front matter © 2007 Elsevier B.V. All rights reserved.
doi:10.1016/j.jpowsour.2007.06.164

Nomenclature

a	Specific surface area of electrode, cm^2/cm^3
A	Geometric area of electrode, cm^2
c	Concentration, mol/cm^3
E	Cell voltage, V
f	Constant, $37.44\,V^{-1}$
F	Constant, 96,487 C/mol
i	Current density, A/cm^2
i_0	Exchange-current density, A/cm^2
I_{app}	Cell current, A
k	Rate-constant, A/cm^2
L	Cathode thickness, cm
m	Mix-ratio
M	Mass, g
n	Number of electron transferred
R	Particle radius, cm
s	Stoichiometric coefficient
t	Time, s
U	Open-circuit voltage, V
V	Cathode volume, cm^3
$\hat{V}$	Molar volume, cm^3/mol

Greek Symbols

β	Transfer-coefficient
θ	Depth of discharge
ρ	Macroscopic density, g/cm^3

Subscripts

C	CF_x
S	SO
SV	SVO
V	VO

Superscripts

max	Maximum
0	Initial

4. Cathode active material is always accessible to the electrolyte regardless of shape changes during discharge.
5. Effects of heat generation, degradation, and parasitic reactions are negligible.
6. Spherical CF_x particles and cylindrical SVO particles.

2.1. Pure CF_x battery

Based on observations presented in the literature [5–7] it is hypothesized that for the discharge rates considered here the CF_x electrode operates under kinetic/charge-transfer limitation only. The overall electrochemical reaction occurring at the cathode is

$$CF_x + xLi^+ + xe^- \rightarrow xLiF + C \quad (1)$$

Since the above reaction is irreversible, the rate of the reaction or current is expressed using Tafel kinetics as

$$i_C = -i_{0C} e^{-\beta_C n_C f(E-U'_C)} \quad (2)$$

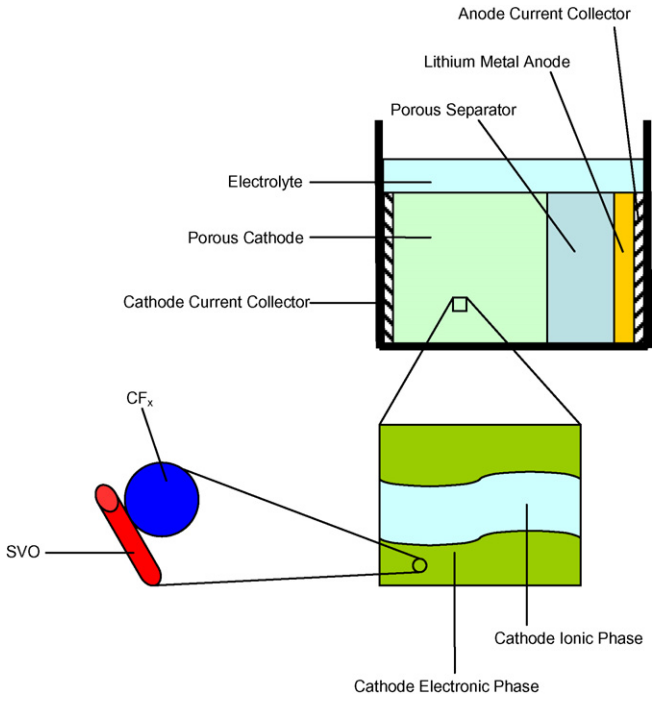

Fig. 1. Schematic of a CF_x–SVO hybrid-cathode battery.

where i_C is the local reaction current density in the porous CF_x electrode, i_{0C} is the exchange-current density of CF_x, β_C is the transfer coefficient of the reaction, n_C is the number of electrons transferred, U_C is the DOD-dependent open-circuit potential of CF_x versus Li, and E is the cell voltage under a load current of I_{app}.

Since a kinetically limited porous electrode operates with a uniform reaction current throughout its volume, the local reaction current density is related to the total cell current by

$$I_{app} = i_C a_C V \quad (3)$$

where

$$a_C V = a_C^0 V^0 (1-\theta_C)^{2/3} \quad (4)$$

The initial total surface area of CF_x, $a_C^0 V^0$, is calculated from the relation

$$a_C^0 V^0 = \frac{3M_C^0}{R_C^0 \rho_C} \quad (5)$$

where M_C^0 and R_C^0 are the initial mass and particle radius of CF_x and ρ_C is the macroscopic density of CF_x in the cathode.

Mass balance with Faraday's law gives the equation governing the variation of DOD with time as

$$\frac{d(1-\theta_C)}{dt} = \frac{d(M_C/M_C^0)}{dt} = -\frac{s_C \hat{V}_C \rho_C}{n_C F M_C^0} i_C a_C V \quad (6)$$

which means that the rate of consumption of CF_x (i.e., the left-hand side) is proportional to the local reaction current density of CF_x. Considering that DOD is zero at the beginning of discharge, the initial condition is set as

$$\text{at } t = 0, \quad \theta_C = 0 \quad (7)$$

Rearranging Eq. (2) and using Eq. (3) and (4), we get an expression for cell voltage as

$$E = U_C - \frac{1}{\beta_C n_C f} \ln\left(\frac{-I_{app}}{(1-\theta_C)^{2/3}}\right) \quad (8)$$

where

$$U_C = U'_C + \frac{1}{\beta_C n_C f} \ln(a_C^0 V^0 i_{0C}) \quad (9)$$

2.2. Pure SVO battery

According to Crespi et al. [4], the overall reaction occurring at the SVO electrode is

$$Ag_2^+V_4^{5+}O_{11} + (x+y)Li^+ + (x+y)e^- \rightarrow Li_{x+y}^+Ag_{2-x}^+V_y^{4+}V_{4-y}^{5+}O_{11} + xAg^0 \quad (10)$$

in which Li insertion is accompanied by silver and vanadium reductions. The open-circuit potential versus DOD curve measured for SVO has two plateaus – one at 3.2 V, corresponding to the phase-change reduction of Ag^+ to Ag and the other at 2.6 V, corresponding to the reduction of V^{5+} to V^{4+}. Further, SVO discharge data shows very different resistances associated with these two regions of the voltage curve. To incorporate these effects in the model, the SVO reduction reaction is treated mathematically as if it is a parallel combination of the reduction reaction of silver as given by

$$Ag_2^+V_4^{5+}O_{11} + xLi^+ + xe^- \rightarrow Li_x^+Ag_{2-x}^+V_4^{5+}O_{11} + xAg^0 \quad (11)$$

and the reduction of vanadium as given by

$$Ag_2^+V_4^{5+}O_{11} + yLi^+ + ye^- \rightarrow Li_y^+Ag_2^+V_y^{4+}V_{4-y}^{5+}O_{11} \quad (12)$$

It is important to note that these reactions may take place simultaneously. Although a simplification, this approach allows for accurate computation of the kinetic resistance associated with SVO reduction.

The overall DOD of the SVO electrode is defined as the sum of the DODs, θ_S and θ_V, of SO and VO reductions. These individual DODs are defined as the values that x and y can take in reactions (11) and (12), respectively, at any time during discharge. In a fully charged SVO electrode, these values are zero and in a fully discharged electrode θ_S reaches 2 and θ_V reaches 5. Note that any side-reaction (e.g., solvent reduction) that may occur near the tail of the voltage curve is lumped together with vanadium reduction.

Assuming purely kinetic limitations, we express the local reaction current density using the Butler–Volmer equation as

$$i_{SV} = i_{0S}[e^{\beta_S n_S f(E-U_S)} - e^{-(1-\beta_S)n_S f(E-U_S)}] + i_{0V}[e^{\beta_V n_V f(E-U_V)} - e^{-(1-\beta_V)n_V f(E-U_V)}] \quad (13)$$

where β_S, i_{0S} and β_V, i_{0V} are the transfer coefficients and exchange-current densities of SO and VO reductions, respectively. U_S and U_V are the DOD-dependent open-circuit potentials for silver and vanadium reductions, respectively.

The local reaction current densities are related to the total cell current by the relation

$$I_{app} = i_{SV} a_{SV} V \quad (14)$$

where a_{SV} is the electrochemically active surface area of SVO per unit volume of the electrode. The quantity $a_{SV}V$ is a constant throughout discharge since SVO is not consumed. It is calculated from the relation

$$a_{SV}V = \frac{2M_{SV}^0}{R_{SV}^0 \rho_{SV}} \quad (15)$$

Mass balance with Faraday's law gives the equation governing the variation of DODs with time as

$$\frac{d\theta_S}{dt} = -\frac{2s_S}{n_S F c_{SV}^{max} R_{SV}^0} i_{0S}[e^{\beta_S n_S f(E-U_S)} - e^{-(1-\beta_S)n_S f(E-U_S)}] \quad (16)$$

$$\frac{d\theta_V}{dt} = -\frac{2s_V}{n_V F c_{SV}^{max} R_{SV}^0} i_{0V}[e^{\beta_V n_V f(E-U_V)} - e^{-(1-\beta_V)n_V f(E-U_V)}] \quad (17)$$

which means that the rate of reaction of Li^+ (i.e., the left-hand side) is proportional to the local reaction current density of SVO. Considering that the SVO electrode is fully charged, we get the initial conditions as

$$\text{at } t = 0, \quad \theta_S = 0 \quad (18)$$

and

$$\text{at } t = 0, \quad \theta_V = 0 \quad (19)$$

Eqs. (13–19) are solved numerically to obtain the cell voltage.

2.3. CF_x–SVO hybrid battery

The electrochemical reactions involved in the CF_x–SVO hybrid cathode are reaction (1) for CF_x and reaction (10) for SVO. Therefore, the kinetic expressions used here are the same as in the pure-component models: Eqs. (2) and (4) for CF_x and Eq. (13) for SVO.

In contrast to the pure-component models presented above, the total reaction current in a hybrid cathode is the sum of the reaction currents of CF_x and SVO. Applying charge balance, the local reaction current densities are related to the total cell current by the relation

$$I_{app} = i_C a_C V + i_{SV} a_{SV} V \quad (20)$$

As with kinetics, the mass balance equations for a hybrid cathode are the same as those for the pure-component models: Eqs. (6 and 7) for CF_x and Eqs. (16–19) for SVO.

Eqs. (2,4–7) and Eq. (13,15–19) are numerically solved with Eq. (20) to obtain the cell voltage.

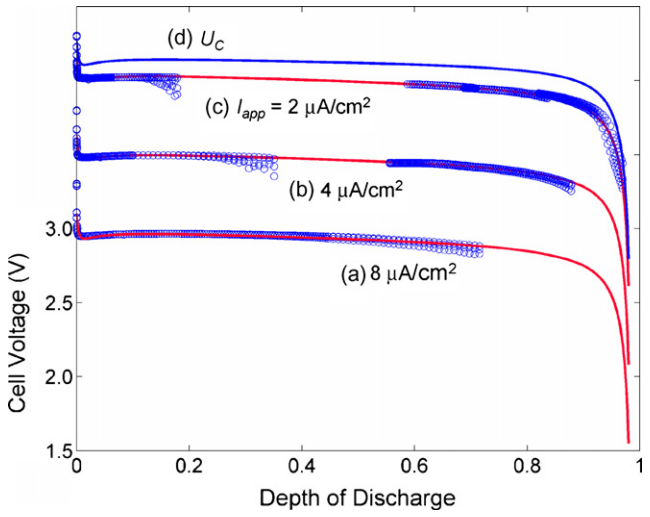

Fig. 2. Model-data comparison for a pure CF_x battery. For clarity, curve (b) is shifted up by 0.5 V and curves (c) and (d) by 1 V.

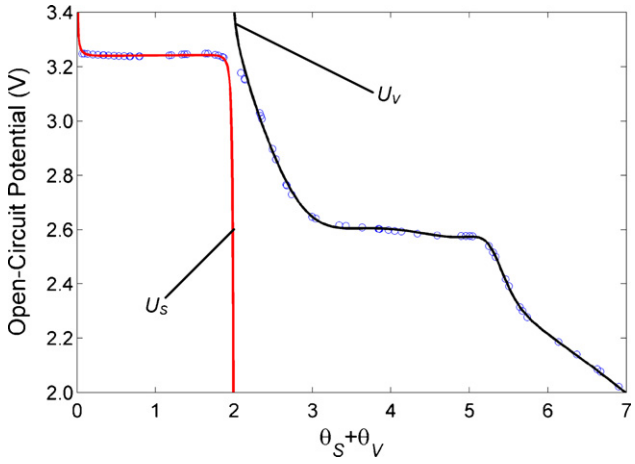

Fig. 3. Measured OCP of SVO reported by Crespi et al. [4] (circles). This OCP curve is split into the OCPs for silver and vanadium reductions, U_S and U_V, and fitted as functions of DOD, θ_S and θ_V, respectively.

3. Model validation and parameter estimation

3.1. Pure CF_x battery

Eq. (8) gives the predicted relationship between cell voltage and DOD for a pure CF_x battery. Fig. 2 shows the comparison between this equation and experimental data obtained from prototype CF_x batteries (circles). The figure shows that the model and data agree well over a range of discharge currents and DODs.

In Eq. (8) two parameters are not known, namely, U_c and the transfer-coefficient, β_C. These parameters are estimated from experimental data by trial-and-error. For a trial value of β_C, Eq. (8) is used to calculate U_c from measured voltage–DOD curves at each rate and plotted. Since this term is current-independent, the right value of β_C should produce the best alignment of these curves. Such a curve of best alignment gives U_c as shown by line (d) in Fig. 2. The value of β_C that produced this curve is 0.57.

3.2. Pure SVO battery

Fig. 3 shows the open-circuit potential curve measured by Crespi et al. [4] as a function of the quantity $x+2y$ of reaction (10), which is equivalent to the sum of the DODs of the silver and vanadium reduction reactions, $\theta_S+\theta_V$. This curve is split into two curves – one spanning the region 0–2 on the x-axis and the other spanning 2–7. The first part is treated as the open-circuit potential for the hypothetical silver reduction (i.e., reaction (11)) and fit as a function of its DOD, θ_S, ranging from 0 to 2. The second part is treated as the open-circuit potential for the hypothetical vanadium reduction (i.e., reaction (12)) and fit as a function its DOD, θ_V, ranging from 0 to 5.

This model is validated by comparing against experimental data obtained on prototype SVO batteries as shown in Fig. 4. The unknown parameters involved are the transfer-coefficients and the exchange-current densities, β_S, i_{0S} and β_V, i_{0V}. The values of the transfer-coefficients do not affect the voltage–capacity curves significantly and, therefore, they are set to 0.5. The measured voltage at the lower plateau shows little change with current, which means that the resistance of vanadium reduction is small. This gives a lower limit of 10^{-4} A/m^2 for i_{0V}. The upper plateau, however, varies strongly with current, which is fitted to obtain i_{0S}. A constant value of i_{0S} does not fit the data and, therefore, the parameter was allowed to vary with θ_S as

$$i_{0S} = k_S(\theta_S^{\max} - \theta_S)^2 \tag{21}$$

The functional form of i_{0S} and the value of k_S are obtained by fitting the higher-voltage plateau. A value of 10^{-6} A/m^2 for k_S produces a good fit. Good overall agreement is obtained between model (lines) and data (circles) over a range of discharge currents.

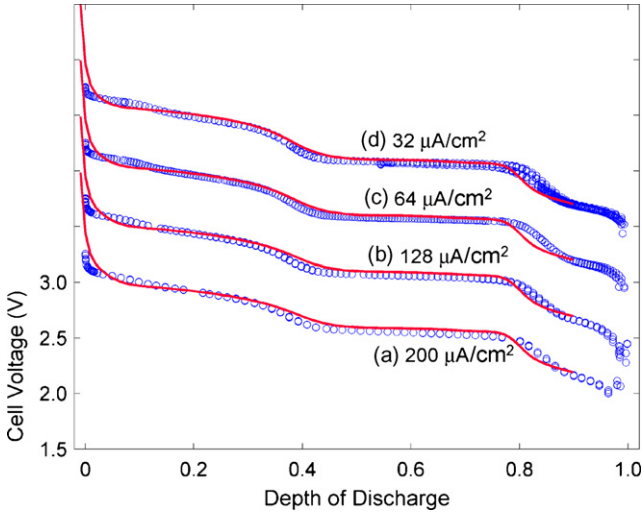

Fig. 4. Model-data comparison for a pure SVO battery. For clarity, curves (b), (c) and (d) are shifted up by 0.5, 1.0 and 1.5 V, respectively.

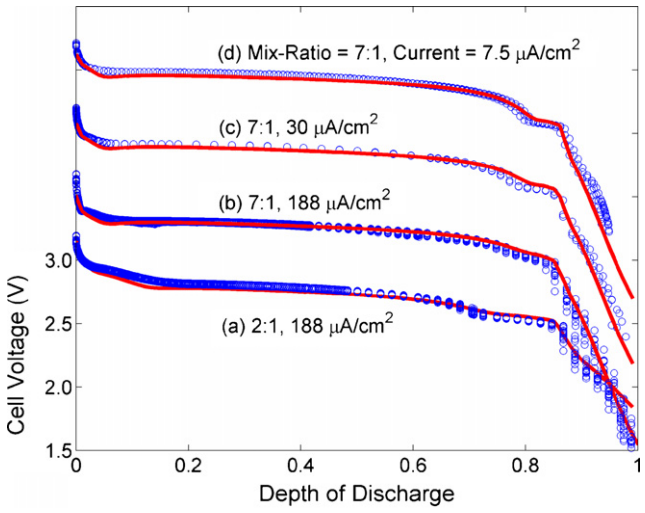

Fig. 5. Model-data comparison for CF_x-SVO hybrid batteries. For clarity, curves (b), (c), and (d) are shifted up by 0.5, 1.0 and 1.5 V, respectively.

3.3. CF_x–SVO hybrid battery

The parameters estimated above with pure CF_x and pure SVO batteries are used here with no other new parameters. The predictions of the model are compared against experimental discharge data obtained from various prototype hybrid batteries varying in cathode thickness, geometric area, and mix-ratio.

As Fig. 5 shows good agreement is obtained between model predictions (lines) and experimental data (circles) for the range of battery designs and discharge currents considered.

4. Conclusion

Physically based mathematical models are developed here for CF_x–SVO hybrid batteries operating at moderate rates. The models are validated by demonstrating good agreement with experimental data over a wide range of design parameters and operating conditions. In the process, key parameters governing kinetic and ohmic resistances in the battery are estimated.

References

[1] D.J. Weiss, J.W. Cretzmeyer, A.M. Crespi, W.G. Howard, P.M. Skarstad, U.S. Patent 5,180,642 (1993).
[2] K. Chen, D.R. Merritt, W.G. Howard, C.L. Schmidt, P.M. Skarstad, J. Power Sources 162 (2006) 837.
[3] D. Merritt, W. Howard, C. Schmidt, P. Scarstad, Meeting abstract, Electrochem. Soc. 502 (831) (2006).
[4] A. Crespi, C. Schmidt, J. Norton, K. Chen, P. Skarstad, J. Electrochem. Soc. 148 (2001) A30.
[5] T. Nakajima, N. Watanabe, Graphite Fluorides and Carbon-Fluorine Compounds, CRC Press, 1991.
[6] W. Tiedemann, J. Electrochem. Soc. 121 (1974) 1308–1311.
[7] S. Davis, E.S. Takeuchi, W. Tiedemann, J. Newman, J. Electrochem. Soc. 154 (2007) A477.